Received: 18 February 2020 | Revised: 27 March 2020 | Accepted: 20 April 2020

DOI: 10.1002/jobm.202000112

RESEARCH PAPER

Journal of Basic Microbiology

Increased Cd^{2+} biosorption capability of *Aspergillus nidulans* elicited by *crpA* deletion

Imre Boczonádi[1,2] | Zsófia Török[3] | Ágnes Jakab[1] | Gábor Kónya[1] | Klaudia Gyurcsó[1] | Edina Baranyai[4] | Zoltán Szoboszlai[3] | Boglárka Döncző[3] | István Fábián[5,6] | Éva Leiter[1] | Mi-Kyung Lee[7] | László Csernoch[8] | Jae-Hyuk Yu[9,10] | Zsófia Kertész[3] | Tamás Emri[1] | István Pócsi[1]

[1]Department of Molecular Biotechnology and Microbiology, Institute of Biotechnology, Faculty of Science and Technology, University of Debrecen, Debrecen, Hungary

[2]Juhász-Nagy Pál Doctoral School, University of Debrecen, Debrecen, Hungary

[3]Laboratory for Heritage Science, Institute for Nuclear Research, Hungarian Academy of Sciences (ATOMKI), Debrecen, Hungary

[4]Department of Inorganic and Analytical Chemistry, Agilent Atomic Spectroscopy Partner Laboratory, University of Debrecen, Debrecen, Hungary

[5]Department of Inorganic and Analytical Chemistry, University of Debrecen, Debrecen, Hungary

[6]MTA-DE Redox and Homogeneous Catalytic Reaction Mechanisms Research Group, Faculty of Science and Technology, University of Debrecen, Debrecen, Hungary

[7]Biological Resource Center, Korea Research Institute of Bioscience and Biotechnology (KRIBB), Daejon, Republic of Korea

[8]Department of Physiology, Faculty of Medicine, University of Debrecen, Debrecen, Hungary

[9]Department of Bacteriology, University of Wisconsin, Madison, Wisconsin

[10]Department of Systems Biotechnology, Konkuk University, Seoul, Republic of Korea

Correspondence
István Pócsi, Department of Molecular Biotechnology and Microbiology, Faculty of Science and Technology, University of Debrecen, Egyetem tér 1, H-4032 Debrecen, Hungary.
Email: pocsi.istvan@science.unideb.hu

Funding information
Higher Education Institutional Excellence Program, Grant/Award Number: NKFIH-1150-6/2019; European Union and the European Social Fund, Grant/Award Number: EFOP–3.6.1–16–2016–00022

Abstract

The P-type ATPase CrpA is an important Cu^{2+}/Cd^{2+} pump in the Aspergilli, significantly contributing to the heavy metal stress tolerance of these ascomycetous fungi. As expected, the deletion of *crpA* resulted in Cu^{2+}/Cd^{2+}-sensitive phenotypes in *Aspergillus nidulans* on stress agar plates inoculated with conidia. Nevertheless, paradoxical growth stimulations were observed with the Δ*crpA* strain in both standard Cu^{2+} stress agar plate experiments and cellophane colony harvest (CCH) cultures, when exposed to Cd^{2+}. These observations reflect efficient compensatory mechanisms for the loss of CrpA operating under these experimental conditions. It is remarkable that the Δ*crpA* strain showed a 2.7 times higher Cd biosorption capacity in CCH cultures, which may facilitate the development of new, fungal biomass-based bioremediation technologies to extract harmful Cd^{2+} ions from the environment. The nullification of *crpA* also significantly changed the spatial distribution of Cu and Cd in CCH cultures, as

demonstrated by the combined particle-induced X-ray emission and scanning transmission ion microscopy technique. Most important, the centers of gravity for Cu and Cd accumulations of the Δ*crpA* colonies shifted toward the older regions as compared with wild-type surface cultures.

KEYWORDS

heavy metals, ICP-OES, ion transport, stress response, PIXE

1 | INTRODUCTION

The removal of heavy metal ions, such as Cd^{2+} and Cu^{2+}, from contaminated soil or wastewater, is essential to avoid their adverse health and environmental effects observable especially at high concentrations. It is clear that Cd^{2+} ions are not transformed into less toxic products in the environment, which explains its bioaccumulation in plants and animals [1]. Cadmium entering the human body through the gastrointestinal and respiratory systems may cause serious damages to all organs including the kidneys, the skeletal muscle, and the liver, which may diminish respiratory function and also elicit nervous disorders [1,2]. Copper is a biologically active essential metal, because some important metalloenzymes like cytochrome oxidase and superoxide dismutase need Cu^{2+} ions for their activity, but exposure to high concentrations of copper may be harmful [3–5].

Various abiotic and biotic technologies have been developed and tested to remove these heavy metal ions from contaminated soil or wastewater. In recent years, research has been focused on the elaboration of novel biosorption-based environmental technologies using promising, effective, and environment-friendly microorganisms [6–8].

Filamentous fungi belonging to the genus *Aspergillus* can tolerate various heavy metal ions, even when they are present at high concentration levels [5,9,10], because *Aspergillus* spp. have adopted several different strategies to resist heavy metal stress as well as to capture and, hence, extract these poisonous ions from the environment [5]. For example, *Aspergillus* spp. possess several protein classes to bind metal ions intracellularly like metallothioneins and others to stabilize and regulate metal homeostasis such as metal ion transporters and metal-binding transcription factors [5,6]. Some heavy metal resistance-associated P-type ATPases play a distinguished role in the control of intracellular concentrations of various heavy metals including Cd^{2+}, Cu^{2+}, and Ag^{+}, and these transporters are evolutionarily conserved and ubiquitously present in bacteria, yeast cells, and filamentous fungi [11].

In the Aspergilli, *Aspergillus nidulans* and *Aspergillus fumigatus* are widespread, saprophytic, and soil-inhabiting molds, which play an essential role in recycling organic materials in the ecological niches occupied by them [5,6]. In addition, *A. nidulans* is a well-known and widely used laboratory model organism, and *A. fumigatus* is a dreadful, opportunistic human pathogen causing serious aspergillosis in the lungs and also systemic mycosis [12]. The third *Aspergillus* species, where Cu^{2+} transporters have been functionally characterized thus far, is *Aspergillus flavus*, an aflatoxin-producing fungus. These highly carcinogenic mycotoxins may enter the feed and food chain, which may cause contaminations dangerous for both livestock and humans [13,14].

In the opportunistic human pathogenic fungus *Candida albicans*, the *CaCRP1* gene encodes a P-type ATPase, which was assigned to the detoxification of Cu^{2+}, Cd^{2+}, and Ag^{+} ions, and which transporter is also required for the virulence of *C. albicans* [15]. More recently, an ortholog of *C. albicans CRP1* has been identified and functionally characterized in *A. fumigatus* (*crpA*; locus ID: AfuA_3g12740), which encodes an efficient Cu^{2+} efflux pump [16,17] and which is also involved in Zn^{2+} detoxification [18]. CrpA is an essential element of the defense mechanism of *A. fumigatus* against alveolar macrophages [16]. Most important, the expression of both *A. nidulans* (locus ID: AN3117) and *A. fumigatus crpA* is under the control of the Cu^{2+}-responsive transcription factor AceA [17–19]. The genome of the crossover pathogen *A. flavus* harbors two *A. fumigatus crpA* homologs called *crpA* (locus ID: AFL2T_03712) and *crpB* (locus ID: AFL2T_10544), whose deletion caused higher Cu^{2+}sensitivity than the lack of AceA [20]. The double gene deletion strain *A. flavus* Δ*crpA*Δ*crpB* colonized maize, as effectively as the wild-type control strain, but a significantly reduced virulence was recorded in a mouse invasive aspergillosis model [20].

In *A. nidulans*, the loss of *crpA* also causes distorted colony morphology under Cu^{2+} stress, with low cellular density in the central regions and, at higher copper concentrations, even extremely thin mycelial mats with individually growing hyphae, which was previously called as “copper phenotype” by Antsotegi-Uskola et al. [19]. *A. nidulans* CrpA localizes primarily in the plasma membrane, but at longer Cu^{2+} exposures, it also appears

in versatile dispersed subcellular structures [19]. CrpA seems to be a Cu^{2+} transporter with some Ag^{+} pumping capability, and it can also export Cd^{2+} ions into the extracellular space when the primary Cd^{2+} detoxification systems (e.g., glutathione-dependent detoxification) are exhausted [19].

In the present study, we further investigated the physiological roles of the CrpA transporter via generating *A. nidulans* Δ*crpA* strains and exposing them to Cu^{2+} and Cd^{2+} stress. In mycelial mats of a selected Δ*crpA* mutant, which were pregrown on cellophane sheets under unstressed conditions, we found a remarkably increased Cd^{2+} biosorption capability after transferring them to stress agar plates supplemented with a high 0.3-mM $CdCl_2$ concentration. We also mapped and visualized the altered spatial distributions of the Cu^{2+} and Cd^{2+} ions within cellophane surface cultures of the *A. nidulans* wild-type and Δ*crpA* mutant strains, using particle-induced X-ray emission (PIXE) and scanning transmission ion microscopy (STIM) accelerator-based ion beam analytical methods.

2 | MATERIALS AND METHODS

2.1 | Strains and culture conditions

In this study, the *A. nidulans* TNJ36 (*pyrG89 AfpyrG*$^{+}$ *pyroA4 veA*$^{+}$) control strain as well as Δ*crpA* (*pyrG89*; Δ*crpA*: *AfupyrG*$^{+}$; *pyroA4*; *veA*$^{+}$) gene deletion mutants were used. The strains were cultured on Barratt's minimal nitrate medium (MNM, supplemented with 0.05% [vol/vol] pyridoxin) at 37°C for 6 days, and the freshly grown conidia were harvested and used in the forthcoming experiments [21]. Most important, MNM is a chemically defined medium, which contains only 0.006-mM Cu^{2+} supplemented with a complex trace element solution [21].

2.2 | Construction of the *A. nidulans* and *A. fumigatus* Δ *crpA* gene deletion strains

The *A. nidulans* AN3117 locus encoding the CrpA transporter in this fungus was deleted by the double-joint polymerase chain reaction (PCR) method of Yu et al. [22,23], using the primers listed in Table S1. The amplified deletion cassette was used to transform RJMP1.59 strain using the Vinoflow FCE lysing enzyme [24]. Single-copy transformants were selected after PCR analysis [25], and three of the transformants lacking the *crpA* gene (MKL5, MKL10, and MKL14) were chosen for stress physiological experiments.

2.3 | Testing the growth inhibitory effects of metal ions

Metal stress sensitivity assays were performed on solid MNM plates, which were supplemented with 0.05–0.5 mM $CuCl_2$ or 0.1–6.0 mM $CdCl_2$, and which were then inoculated with 5 μl of conidial suspension (1×10^5 conidia) and incubated at 37°C for 5 days as per previous standardized protocols [9,10]. Fungal growth values (mean ± *SD*) were determined from three independent experiments for each heavy metal treatment. Fungal growth was characterized by colony diameters, and metal stress sensitivities were quantified by percentage decreases in the colony growth as compared with the appropriate control cultures [9,10].

2.4 | Measuring cadmium and copper contents of *A. nidulans* TNJ36 control and MKL14 Δ *crpA* mutant strains using inductively coupled plasma optical emission spectrometry

The cellophane colony harvest (CCH) method [26,27] was used for heavy metal elemental analyses. Both the TNJ36 control and the MKL14 Δ*crpA* strains were point-inoculated (with 1×10^5 conidia in 5 μl suspensions) into MNM agar plates covered by sterile and semipermeable cellophane sheets. After 24-h incubation at 37°C, the pregrown mycelial mats were transferred into freshly prepared stress agar plates supplemented with 0.1–0.4 mM $CuCl_2$ or 0.1–0.5 mM $CdCl_2$, as required, and then incubated further at 37°C for 5 days. Then, relative growth values (means ± *SD* values calculated from three independent measurements) were determined, as described above for the stress experiments.

Cellophane sheets with heavy metal ion-exposed mycelial mats were removed from the surface of MNM agar, and fungal mycelia were harvested with spatula, frozen immediately at −70°C, and freeze-dried overnight in a CHRIST Alpha 1-2 LDplus lyophilizer (Osterode, Germany) [27]. Then, the metal contents of the biomass samples were determined by inductively coupled plasma optical emission spectrometry (ICP-OES; 5100 Agilent Technologies, Santa Clara, CA) following atmospheric wet digestion in 65% (M/M) HNO_3 and 0.5-ml, 30% (M/M) H_2O_2 in glass beakers. Using ICP-OES elemental analysis data, metal contents of the biomasses were calculated and expressed in mg/kg units, as described elsewhere [28].

2.5 | Elemental analysis of fungal biomass samples by PIXE–STIM

For PIXE–STIM elemental analyses, we also used the CCH cultures of the TNJ36 control and the MKL14 Δ*crpA*

strains [26,27]. Nevertheless, in this case, we did not separate mycelial mats from the cellophane sheets. Instead, whole CCH specimens (mycelia on sheets) were frozen (−70°C), lyophilized, and Petri dishes covered by sealing film were transported at 4°C to the PIXE–STIM laboratory without delay.

The PIXE measurements were carried out at the scanning nuclear microprobe facility at the 0° beamline of the 5-MV Van de Graaff accelerator located at ATOMKI, Debrecen, Hungary [29,30]. Narrow rectangles (0.5 cm) of the mycelial mats were cut out by scalpels, starting from the point of inoculation to the edges of the colonies, and they were fit into grids (2.0 cm); a proton beam of 2.5-MeV energy focused down to ~2 μm × 2 μm, and 200–300 pA current was used to irradiate the samples.

For the characterization of the fungal mycelial mats, a measurement setup developed for biomedical applications [31], using a combination of ion beam analytical techniques, was applied. PIXE technique was used to measure the elemental composition of the samples for $Z > 5$, whereas STIM method provided information about the morphology, surface density, and thus the thickness of the samples. The measurement setup consisted of two X-ray detectors, placed at 135° geometry to the incidence beam, a surface barrier PIPS particle detector, and a beam chopper. An SDD detector with AP3.3 ultra-thin polymer window (SGX Sesortech) with 30-mm^2 active surface area was used to measure low- and medium-energy X-rays (0.2–12 keV, $Z > 5$), whereas a Gresham-type Be Windowed Si(Li) X-ray detector with 30-mm^2 active surface area equipped with an additional Kapton filter of 125-μm thickness was applied to detect the medium- and high-energy X-rays (3–30 keV, $Z > 19$) [30]. For STIM measurements, a Canberra-type PIPS particle detector (11-keV nominal energy resolution) with 50-mm^2 active area was used both in on-axis and off-axis geometries. The beam dose was measured with a beam chopper and with a Faraday cup behind the sample [32]. Signals from all detectors were recorded event by event in list mode by the Oxford-type OMDAQ data acquisition system [33]. Elemental maps of a 1.5-mm × 1.5-mm area were recorded through the entire length of the freeze-dried samples. Such a 1.5-mm × 1.5-mm area represented one spot. In a sample, 6–9 spots were selected for measurement, equally distributed between the edges and centers of the colonies. During the analysis, we excluded spots at the very edges where the cellophane sheets were not fully covered by mycelial mats yet, that is, where the confluency was less than 100%. To protect the particle detector from radiation damage, STIM measurements in on-axis geometry were performed with a beam current of 500–1,000 protons/s.

The obtained PIXE spectra were evaluated with the GUPIXWIN program code [34]. The simplest case for the evaluation of PIXE spectra is when the major elemental content (i.e., those that constitute ~90–99% of the sample, the so-called matrix) is known, and GUPIX solves in a simple and direct fashion to determine the desired trace element concentrations in that known matrix. The thickness of the samples and the energy loss of the irradiating beam due to the transmission through the samples were determined from the STIM measurements. The samples were treated as "intermediate thick" samples. The light element components (H, C, N, O, and S—the matrix) of the dried and harvested biomass samples were determined by an Elementar Vario Micro analyzer (Hanau, Germany; Table S2).

On the spectra of both PIXE detectors, the X-ray energy range of 3.0–8.5 keV is common; therefore, intensive X-ray lines within this range (e.g., Ca K_α, K K_α), were used to normalize the elemental concentrations. In most cases, the differences of the concentration values of the two detectors were between 0% and 5%. The following elements were fitted: O, Na, Mg, Al, Si, P, S, Cl, K, Ca, Ti, V, Cr, Mn, Fe, Cu, Zn, and Cd. The uncertainty of the PIXE measurement for the main components is ~25%, whereas for the trace elements, it is ~10–15%. Concentration values were expressed in μg/(g DCM).

To check the quality and precision of the dose measurement and the determination of the concentrations, measurements on standard reference materials (SRMs) were carried out. SRMs used for the validation were the following: A series of pure metals (Zn, Sn, Ti, Ta) and layered samples (6-μm-thick Ti foil on 50-μm Ni and 6-μm-thick Ti foil on 8-μm Ta). Layered standards were also used for calibration of the STIM measurements. The calibration of the beam chopper was also done on each measurement day. These measurements help determine the exact measurement conditions (e.g., solid angles of detectors).

3 | RESULTS

Not surprisingly, all *A. nidulans* Δ*crpA* gene deletion strains, constructed and tested (MKL5, MKL10, and MKL14), showed an increased sensitivity to Cu^{2+} ions, when added at least at 0.150-mM concentrations (Figures S1 and S2). Most important, all colonies at and above 0.125-mM Cu^{2+} concentrations showed characteristic "copper phenotype" colony morphologies with thin mycelial mats [19]. In addition, all Δ*crpA* strains showed a significantly increased sensitivity to Cd^{2+} ions, even at as low as 0.1-mM concentration (Figures S3 and S4). It is worth mentioning that each

Δ*crpA* strain including MKL14 showed a significantly increased tolerance to Cu^{2+} stress elicited by 0.125-mM or lower $CuCl_2$ concentrations (e.g., 14.7 ± 4.2% growth stimulation was recorded with the MKL14 strain at 0.1-mM Cu^{2+} concentration; Figure 1). These observations may be indicative that other effective Cu^{2+} detoxification systems were activated in the absence of *crpA*, overcompensating the loss of this important Cu^{2+} pump (Figures 1, S1, and S2).

In CCH cultures of the *A. nidulans* strains, both Cu^{2+} and Cd^{2+} tolerances of the TNJ36 control and the MKL14 Δ*crpA* strains increased considerably as compared with stress agar experiments, which were inoculated by conidia (Figures 1 and 2). It was surprising that no "copper phenotype" [19] appeared under these experimental conditions (Figure 1). Quite unexpectedly, exposures to 0.1–0.5 mM $CdCl_2$ in CCH cultures slightly stimulated the colony growth of the *A. nidulans* MKL14 Δ*crpA* mutant as compared with the control strain; meanwhile, no such phenomenon was observed in standard stress agar experiments where agar plates were inoculated with spore suspensions (Figure 2).

Considering the total cadmium uptakes by the *A. nidulans* TNJ36 control and MKL14 Δ*crpA* gene deletion strains, the Cd-accumulating capability of the mutant in the presence of 0.3-mM $CdCl_2$ was approximately 2.7 times higher than that of the wild-type strain (1672.7 ± 104.7 vs. 612.5 ± 189.3 mg/(kg DCM); Table 1). Most important, the increased Cd^{2+} biosorption potential of the *A. nidulans* MKL14 Δ*crpA* strain seemed to be specific to heavy metal, because the Cu accumulations by the tested TNJ36 and MKL14 strains were comparable with each other at 0.3-mM $CuCl_2$ concentration (Table 1).

The spatial distributions of Cu^{2+} and Cd^{2+} in *A. nidulans* colonies were mapped by PIXE. As indicated above, the TNJ36 control strain grew somewhat better in CCH cultures in the presence of 0.3-mM $CuCl_2$ and the $CdCl_2$ tolerance of MKL14 Δ*crpA* strain exceeded that of the control strain (Figures 1, 2, and S5).

In the case of the 0.3-mM $CuCl_2$-exposed TNJ36 control strain, copper was accumulated evenly after the very edge of the colony (4.5–6 mm from the edge) at a concentration of 1,100 μg/(g DCM) (the uncertainties of the Cu concentrations were about 10%), yet in the middle of

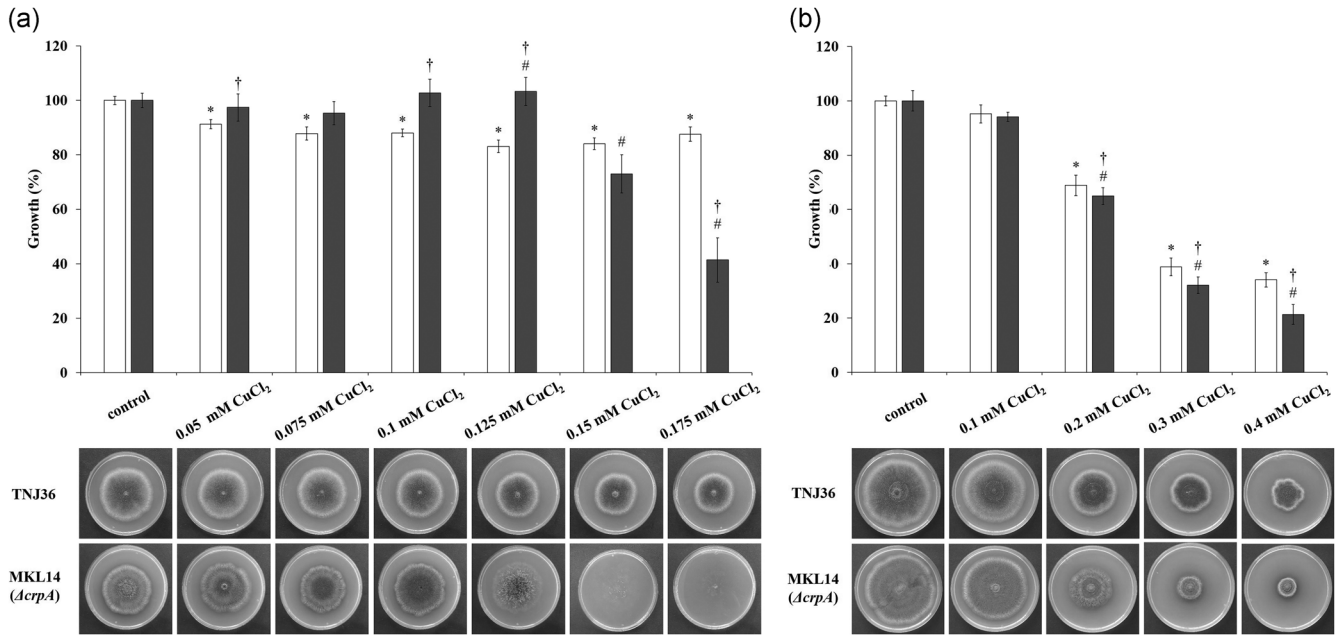

FIGURE 1 Cu^{2+} stress sensitivities of the *Aspergillus nidulans* TNJ36 control and the MKL14 Δ*crpA* gene deletion mutant strains. Stress sensitivities observed in surface cultures on minimal nitrate medium (MNM) stress agar plates (a) and on cellophane-covered MNM stress agar plates (cellophane colony harvest [CCH] cultures; b) are presented. In both cases, conidiospores (10^5 in 5-μl suspensions) were point-inoculated into MNM stress agar or cellophane-covered MNM agar. It should be noted that in the case of the CCH cultures, conidia- were allowed to germinate in the absence of stressors; they were incubated at 37°C for 24 h and were then transferred directly to the surface of stress agar plates. All stress agar plate cultures were incubated at 37°C for 5 days. Mean colony diameters of the control (white columns) and the mutant (gray columns) strains are presented with standard deviation values calculated from three independent experiments, together with a typical set of photos of the stress-exposed cultures. *, #, and † indicate significant differences at $p < .05$ significance level (calculated by Student's *t* test) between treated TNJ36 control versus nontreated TNJ36 control, between treated MKL14 Δ*crpA* versus nontreated MKL14 Δ*crpA*, and between treated MKL14 Δ*crpA* versus treated TNJ36 control strains, respectively

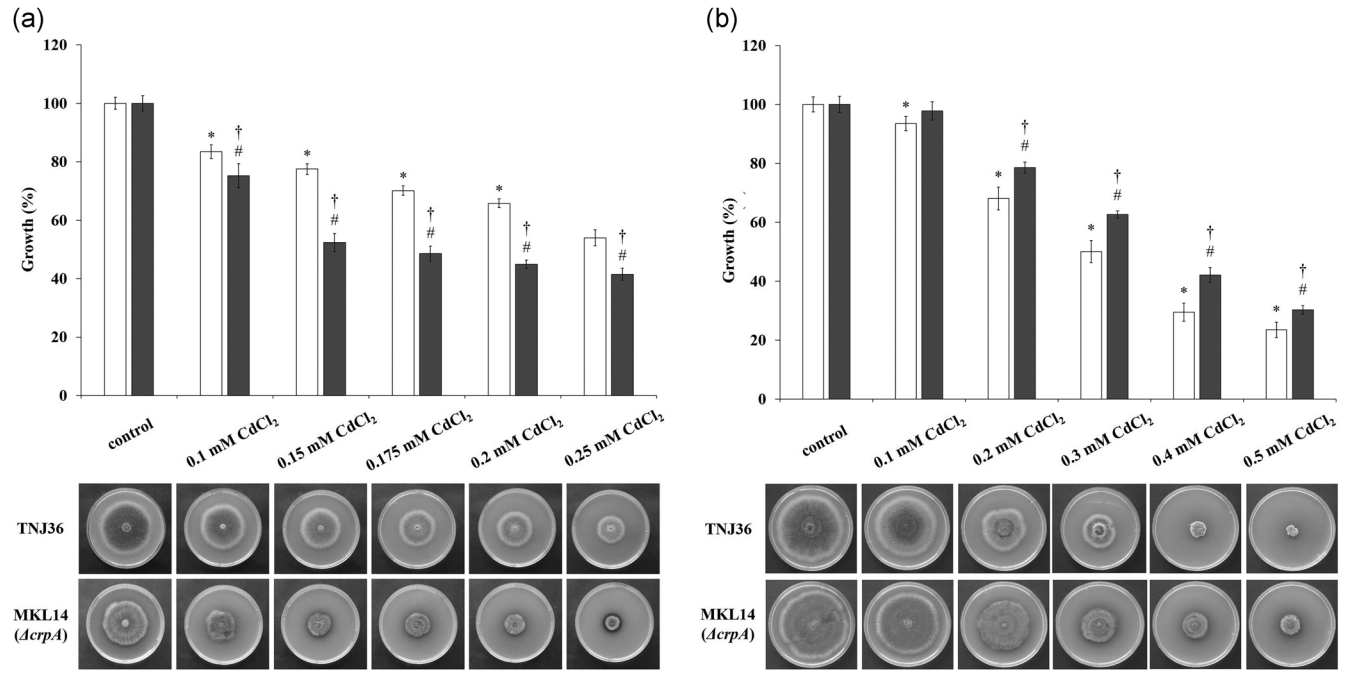

FIGURE 2 Cd^{2+} stress sensitivities of the *Aspergillus nidulans* TNJ36 control and the MKL14 Δ*crpA* gene deletion mutant strains. (a) Stress sensitivities observed in surface cultures on minimal nitrate medium (MNM) stress agar plates are presented, and (b) stress sensitivities recorded on cellophane-covered MNM stress agar plates (cellophane colony harvest [CCH] cultures; b) are shown. The experimental arrangements were the same as described for Cu^{2+} exposures in the legend of Figure 1. *, #, and † indicate significant differences at $p < .05$ significance level (calculated by Student's *t* test) between treated TNJ36 control versus nontreated TNJ36 control, between treated MKL14 Δ*crpA* versus nontreated MKL14 Δ*crpA*, and between treated MKL14 Δ*crpA* versus treated TNJ36 control strains, respectively

the colony (13.5–15 mm), it showed a reduced concentration, 590 μg/(g DCM), toward the aging region (Figure 3). The MKL14 Δ*crpA* gene deletion mutant strain showed a slower, but increasing, copper accumulation dynamics, with the maximum of 1,200 μg/(g DCM) in the metabolically inactive regions (10–13.5 mm), but, similar to the control, the concentration of copper continued to decrease, with the minimum of 870 μg/(g DCM), inside the colony (Figure 3).

The cadmium concentrations were higher, with the maximum of 850 μg/(g DCM) (the uncertainties of the Cd concentrations were about 15%), between the center and the edge of the colony (7.5–9.0 mm; Figure 4). The cadmium concentration showed an increasing tendency from the edge of the colony to the aging region, with the maximum of 1,300 μg/(g DCM) (16.5–19.5 mm from the edge; Figure 4).

TABLE 1 Copper and cadmium adsorptions by *Aspergillus nidulans* TNJ36 control and the Δ*crpA* gene deletion mutant strains

Treatment	Metal contents[a]	
	TNJ36	MKL14 (Δ*crpA*)
+0.3-mM $CuCl_2$	665.6 ± 182.9 (mg/kg)	697.1 ± 106.9 (mg/kg)
	10.5 ± 2.9 (mM/kg)	10.9 ± 1.7 (mM/kg)
+0.3-mM $CdCl_2$	612.5 ± 189.3 (mg/kg)	1672.7 ± 104.7 (mg/kg)*
	5.4 ± 1.7 (mM/kg)	14.9 ± 0.9 (mM/kg)*

[a]Mean metal content ± *SD* values, calculated from three independent experiments, are presented.
*Significant difference at $p < .05$ (calculated by Student's *t* test) between cadmium-exposed control (TNJ36) and Δ*crpA* gene deletion (MKL14) strains.

4 | DISCUSSION

As expected, all Δ*crpA* gene deletion mutants constructed and tested by us (MKL5, MKL10, MKL14) showed increased sensitivities to Cu^{2+} and Cd^{2+} heavy metal stresses (Figures S1–S4). All these observations were in line with previous experimental data published by Antsotegi-Uskola et al. [19], and the MKL14 Δ*crpA* strain was chosen for further stress and analytical studies.

"Copper phenotype" colony morphology (very thin, loose mycelial mats) [19] was only visible in standard stress agar experiments with the Δ*crpA* strains (Figures 1

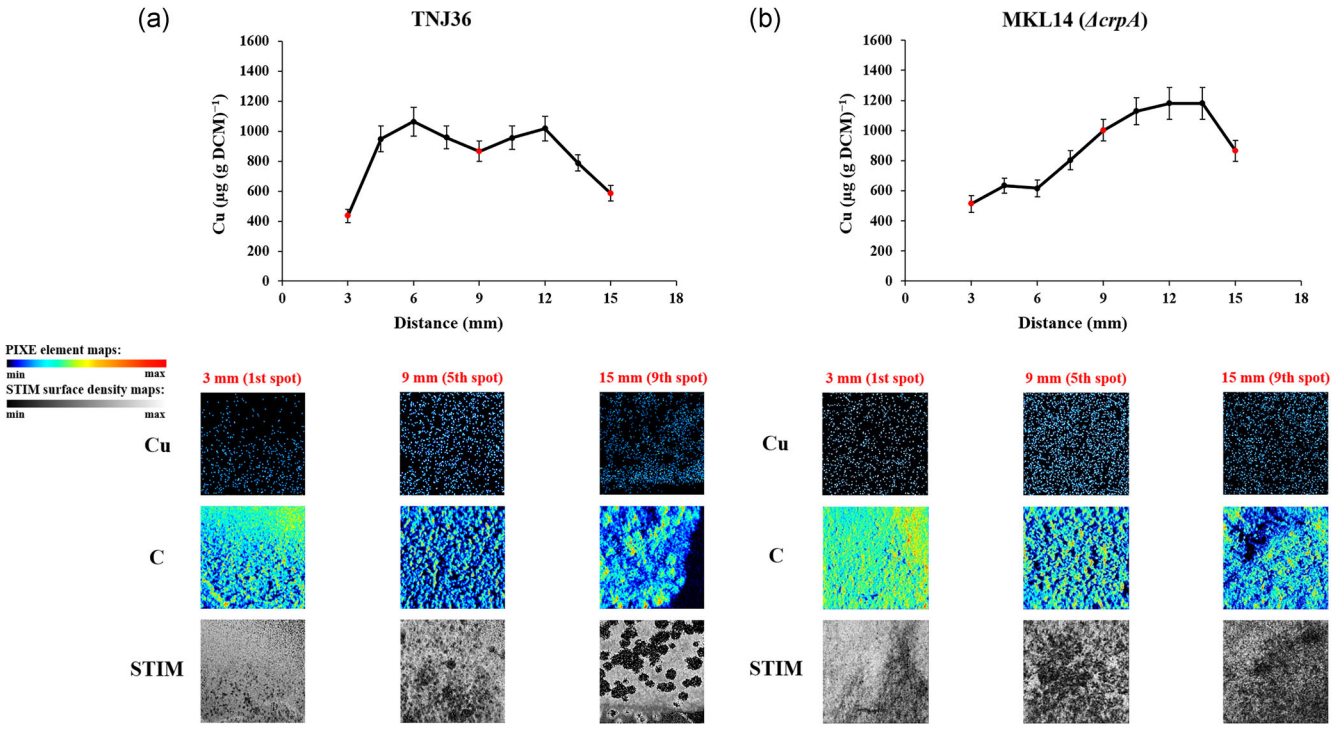

FIGURE 3 The particle-induced X-ray emission (PIXE) elemental analysis of copper distributions in *Aspergillus nidulans* TNJ36 control (a) and MKL14 Δ*crpA* (b) colonies. Changes in Cu distribution observed in colonies of the *A. nidulans* TNJ36 control (a) and the MKL14 Δ*crpA* gene deletion mutant (b) strains. Elemental contents (μg/(g DCM), filled symbols) of 1.5 mm × 1.5 mm areas were measured with PIXE and scanning transmission ion microscopy (STIM) techniques through the freeze-dried samples (in 9 spots), where the origin (point 0) of the *x*-axis was set at the very edge of the colony. Elemental distribution maps (Cu, C) and STIM images recorded at spots 1 (edge, where the cellophane sheet was covered by the mycelial mat with 100% confluency), 7 (between the edge and the middle), and 9 (middle of the colony) are presented. The color scales indicate the variation in elemental contents from the highest concentration in red and white to lowest in blue and black

and S1), and it was absent in CCH cultures of the MKL14 strain (Figure 1), clearly indicating that the appearance of this special phenotype was organically coupled to the germination of Cu^{2+}-exposed mutant conidiospores under high Cu^{2+} concentration.

Most important, CCH cultures of both the TNJ36 and MKL14 strains were more tolerant to both Cu^{2+} and Cd^{2+} stresses than their standard stress agar cultures (Figures 1 and 2). Similar phenomena have been reported previously with *A. nidulans* Δ*atfA* mutants and appropriate control strains in the presence of the lipid peroxidation-initiating compound *tert*-butyl hydroperoxide [26]. The bZIP-type transcription factor AtfA is one of the key regulators of environmental stress response in *A. nidulans* [26,35–37].

Paradoxical stress sensitivity phenotypes with unexpectedly increased heavy metal tolerances were observed in Cu^{2+}-exposed (at concentrations equal to or less than 0.125 mM) standard stress agar cultures of the MKL14 Δ*crpA* strain (Figures 1, S1, and S2), and in Cd^{2+}-exposed MKL14 CCH cultures (Figure 2). According to Antsotegi-Uskola et al. [19], CrpA is primarily a Cu^{2+} transporter, which may also transport Cd^{2+} ions when other major Cd^{2+} detoxification systems (other Cd^{2+} pumps and the glutathione/phytochelatin system) are saturated. In agreement with this hypothesis, overcompensation mechanisms for the loss of the CrpA pump were more effective for Cd^{2+} than for Cu^{2+} ions at least in CCH cultures, resulting in a significantly increased Cd^{2+} tolerance and biosorption (Figure 2 and Table 1). Furthermore, similar overcompensations for lost elements of fungal stress response systems and consequently emerging paradoxical stress tolerance phenotypes have already been published in the literature [38–40]. Further studies are needed to shed light on the molecular background of the overcompensation mechanisms operating in the MKL14 Δ*crpA* mutant under Cd^{2+} exposures, but the upregulation of the biosynthesis of thiol-containing compounds like glutathione and metallothioneins [41–45] and/or alternative Cd^{2+} transporters like PcaA [27,46] should be examined.

The remarkably increased Cd-accumulating capability (1,672.7 ± 104.7 mg/(kg DCM) at 0.3 mM $CdCl_2$; Table 1) of the MKL14 Δ*crpA* strain is outstanding among

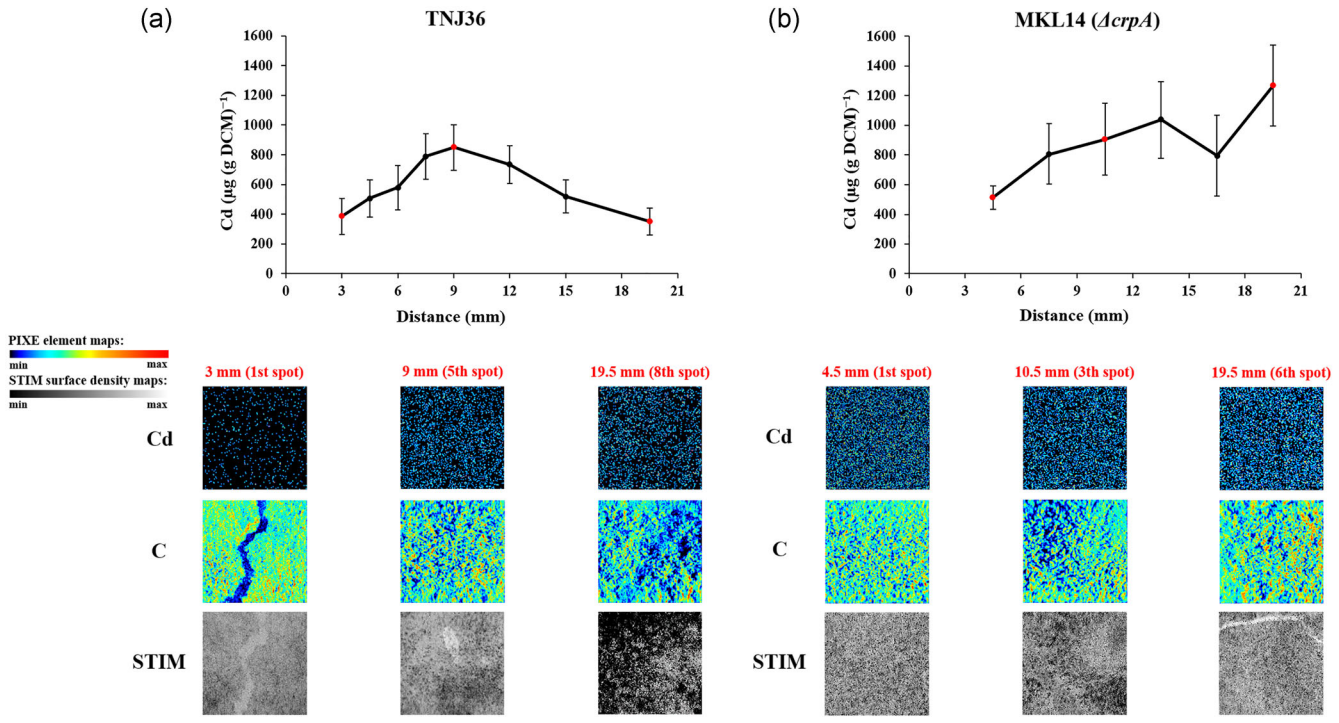

FIGURE 4 The particle-induced X-ray emission (PIXE) elemental analysis of cadmium distributions in *Aspergillus nidulans* TNJ36 control (a) and MKL14 Δ*crpA* (b) colonies. Changes in Cd distribution observed in colonies of the *A. nidulans* TNJ36 control (a) and the MKL14 Δ*crpA* gene deletion mutant (b) strains. Elemental contents (μg/(g DCM), filled symbols) measured in 1.5 mm × 1.5 mm areas using PIXE and scanning transmission ion microscopy (STIM) techniques in 8 (strain TNJ36) or 6 (strain MKL14) spots are presented, where the origin (point 0) of the *x*-axis was set at the very edge of the colony. Elemental distribution maps (Cd, C) and STIM images recorded at spots 1 (edge, where the coverage of the cellophane sheet by mycelia reached 100%), 6 (strain TNJ36) or 4 (strain MKL14; between the edge and the middle), and 8 (strain TNJ36) or 6 (strain MKL14; middle of the colony) are shown. The color scales indicate the variation in elemental contents from highest concentration in red and white to lowest in blue and black

fungi, because the *A. fumigatus* Af293 strain characterized before with a notable Cd^{2+} tolerance [9,10,23,27] accumulated less, 850 ± 110 mg/(kg DCM), Cd when exposed to 2-mM $CdCl_2$ in CCH cultures [27]. It is important to note that Kurucz et al. [27] inoculated cellophane sheets placed on Cd^{2+} supplemented stress agar plates directly with 5-μl suspensions of 1×10^5 *A. fumigatus* spores without any preincubation under unstressed conditions. Nevertheless, the observed remarkable Cd^{2+} tolerance and accumulation of the *A. nidulans* MKL14 Δ*crpA* mutant makes this strain a promising candidate for the development of novel fungal biomass-based Cd^{2+} biosorption technologies [47–49]. In future filamentous fungus-based bioremediation technologies, *A. nidulans* could be superior to *A. fumigatus*, because the latter species is known as the most widespread and most dangerous opportunistic filamentous fungus pathogen to humans [12].

From the spatial heavy metal accumulation patterns based on PIXE–STIM measurements (Figures 3 and 4), we concluded that both heavy metals distributed mostly between the edges and the middle parts of the TNJ36 control strain colonies. It is clear that CrpA, together with other heavy metal ion transporters [16–20,23], actively pumped Cu^{2+} and Cd^{2+} ions out of the cells at apical and subapical regions of hyphae [19,23], which resulted in low Cu^{2+} and Cd^{2+} concentrations at the colony edges (Figures 3 and 4). Alternative detoxification mechanisms like complexation of these ions with metallothioneins (e.g., for Cu^{2+}) [18,19] and glutathione (e.g., for Cd^{2+}) [19,50,51] also contributed to the control and neutralization of these ions. In the MKL14 Δ*crpA* strain, the edges contained less heavy metal ions than the aging parts (Figures 3 and 4), indicating the onset of compensating mechanisms for the loss of CrpA, but the center of gravity for heavy metal accumulation was shifted clearly toward older regions. This is indicative of the activation of alternative intracellular detoxification processes in the MKL14 Δ*crpA* strain, transporting heavy metal ions and their metallothionein and glutathione complexes most likely to the vacuoles of older hyphal segments in addition to biosorption by the cell wall [42,52–55].

By using PIXE–STIM analysis, it is possible to perform quantification of the amounts and distribution of elements in biological and environmental samples [56]. Various types of bacteria, fungal, plant, and human

material have been analyzed using PIXE. Earlier studies have reported the elemental compositions of magnetotactic bacterium [57], heavy metal-accumulating *Citrobacter* sp. [58], *Fusarium culmorum* hyphae exposed to chemical agents [59], fruit bodies of the wood-rotting fungus *Fomes fomentarius* [60], mycorrhizal roots and arbuscular mycorrhizal fungal hyphae and spores [61–67], mycothallic fern [68], living xylem infected by pathogenic fungi [69], and also human samples [70–72].

The clear-cut differences observed in the heavy metal distribution patterns of the *A. nidulans* TNJ36 control and MKL14 Δ*crpA* gene deletion strains using the PIXE–STIM technique in CCH stress agar plate surface cultures (Figures 3 and 4) helped us to gain a deeper insight into the molecular mechanisms behind the increased Cd^{2+} tolerance and biosorption phenotypes. We suggest that such PIXE–STIM measurements could be employed in the future in both basic research and applied research projects when the heavy metal-accumulating potential and mechanism of saprophytic fungi are of paramount interest.

ACKNOWLEDGMENTS

The authors acknowledge the participation of L. G. Tóth (University of Debrecen) in the stress agar plate experiments. This study was supported by the European Union and the European Social Fund through the EFOP–3.6.1–16–2016–00022 project and by the Higher Education Institutional Excellence Program (NKFIH-1150-6/2019) of the Ministry of Innovation and Technology in Hungary, within the framework of the Biotechnology thematic program of the University of Debrecen.

CONFLICT OF INTERESTS

The authors declare that there are no conflict of interests.

ORCID

Imre Boczonádi http://orcid.org/0000-0001-7643-4495
Éva Leiter http://orcid.org/0000-0001-6759-2790
Tamás Emri http://orcid.org/0000-0002-8850-6975
István Pócsi http://orcid.org/0000-0003-2692-6453

REFERENCES

[1] Jaishankar M, Tseten T, Anbalagan N, Mathew BB. Toxicity, mechanism and health effects of some heavy metals. Interdiscip Toxicol. 2014;7:60-72.
[2] Zhou Z, Lu Y, Pi H, Gao P, Li M, Zhang L, et al. Cadmium exposure is associated with the prevalence of dyslipidemia. Cell Physiol Biochem. 2016;40:633-43.
[3] Macomber L, Rensing C, Imlay JA. Intracellular copper does not catalyze the formation of oxidative DNA damage in *Escherichia coli*. J Bacteriol. 2007;189:1616-26.
[4] Cotruvo JA Jr, Aron AT, Ramos-Torres KM, Chang CJ. Synthetic fluorescent probes for studying copper in biological systems. Chem Soc Rev. 2016;44:4400-14.
[5] Gerwien F, Skrahina V, Kasper L, Hube B, Brunke S. Metals in fungal virulence. FEMS Microbiol Ecol. 2018;42:fux050.
[6] Veglio F, Beolchini F. Removal of metals by biosorption: a review. Hydrometallurgy. 1997;44:301-16.
[7] Mani D, Kumar C. Biotechnological advances in bioremediation of heavy metals contaminated ecosystems: an overview with special reference to phytoremediation. Int J Environ Sci Technol. 2014;11:843-72.
[8] Bano A, Hussain J, Akbar A, Mehmood K. Biosorption of heavy metals by obligate halophilic fungi. Chemosphere. 2018;199:218-22.
[9] de Vries RP, Riley R, Wiebenga A, Aguilar-Osorio G, Amillis S, Uchima CA, et al. Comparative genomics reveals high biological diversity and specific adaptation in the industrially and medically important fungal genus *Aspergillus*. Genome Biol. 2017;18:28.
[10] Orosz E, van de Wiele N, Emri T, Zhou M, Robert V, de Vries RP, et al. Fungal Stress Database (FSD)—a repository of fungal stress physiological data. Database. 2018;2018:bay009.
[11] Kühlbrandt W. Biology, structure and mechanism of P-type ATPases. Nat Rev Mol Cell Biol. 2004;5:282-95.
[12] Dagenais TRT, Keller NP. Pathogenesis of *Aspergillus fumigatus* in invasive Aspergillosis. Clin Microbiol Rev. 2009;22:447-65.
[13] Peles F, Sipos P, Győri Z, Pfliegler WP, Giacometti F, Serraino A, et al. Adverse effects, transformation and channeling of aflatoxins into food raw materials in livestock. Front Microbiol. 2019;10:2861.
[14] Ráduly Z, Szabó L, Madar A, Pócsi I, Csernoch L. Toxicological and medical aspects of *Aspergillus*-derived mycotoxins entering the feed and food chain. Front Microbiol. 2020;10:2908.
[15] Riggle PJ, Kumamoto CA. Role of a *Candida albicans* P1-type ATPase in resistance to copper and silver ion toxicity. J Bacteriol. 2000;182:4899-905.
[16] Wiemann P, Perevitsky A, Huttenlocher A, Osherov N, Keller NP. *Aspergillus fumigatus* copper export machinery and reactive oxygen intermediate defense counter host copper-mediated oxidative antimicrobial offense. Cell Rep. 2017;19:1008-21.
[17] Raffa N, Osherov N, Keller NP. Copper utilization, regulation, and acquisition by *Aspergillus fumigatus*. Int J Mol Sci. 2019;20:E1980.
[18] Cai Z, Du W, Zhang Z, Guan L, Zeng Q, Chai Y, et al. The *Aspergillus fumigatus* transcription factor *AceA* is involved not only in Cu but also in Zn detoxification through regulating transporters CrpA and ZrcA. Cell Microbiol. 2018;20:12864.
[19] Antsotegi-Uskola M, Markina-Iñarrairaegui A, Ugalde U. Copper resistance in *Aspergillus nidulans* relies on the PI-type ATPase CrpA, regulated by the transcription factor AceA. Front Microbiol. 2017;8:912.
[20] Yang K, Shadkchan Y, Tannous J, Landero Figueroa JA, Wiemann P, Osherov N, et al. Contribution of ATPase copper transporters in animal but not plant virulence of the crossover pathogen *Aspergillus flavus*. Virulence. 2018;9:1273-86.
[21] Barratt RW, Johnson GB, Ogata WN. Wild-type and mutant stocks of *Aspergillus nidulans*. Genetics. 1965;52:233-46.
[22] Yu JH, Hamari Z, Han KH, Seo JA, Reyes-Domínguez Y, Scazzocchio C. Double-joint PCR: a PCR-based molecular tool for gene manipulations in filamentous fungi. Fungal Genet Biol. 2004;41:973-81.

[23] Bakti F, Király A, Orosz E, Miskei M, Emri T, Leiter É, et al. Study on the glutathione metabolism of the filamentous fungus *Aspergillus nidulans*. Acta Microbiol Immunol Hung. 2017;64:255-72.
[24] Szewczyk E, Nayak T, Oakley CE, Edgerton H, Xiong Y, Taheri-Talesh N, et al. Fusion PCR and gene targeting in *Aspergillus nidulans*. Nat Protoc. 2006;1:3111-20.
[25] Leiter É, Bálint M, Miskei M, Orosz E, Szabó Z, Pócsi I. Stress tolerances of nullmutants of function-unknown genes encoding menadione stress-responsive proteins in *Aspergillus nidulans*. J Basic Microbiol. 2016;56:827-33.
[26] Balázs A, Pócsi I, Hamari Z, Leiter É, Emri T, Miskei M, et al. *AtfA* bZIP-type transcription factor regulates oxidative and osmotic stress responses in *Aspergillus nidulans*. Mol Genet Genomics. 2010;283:289-303.
[27] Kurucz V, Kiss B, Szigeti ZM, Nagy G, Orosz E, Hargitai Z, et al. Physiological background of the remarkably high Cd^{2+} tolerance of the *Aspergillus fumigatus* Af293 strain. J Basic Microbiol. 2018;58:957-67.
[28] Sajtos Z, Herman P, Harangi S, Baranyai E. Elemental analysis of Hungarian honey samples and bee products by MP-AES method. Microchem J. 2019;149:10396.
[29] Rajta I, Borbély-Kiss I, Mórik G, Bartha L, Koltay E, Kiss ÁZ. The new ATOMKI scanning proton microprobe. Nucl Instrum Methods Phys Res. 1996;109–110:148-53.
[30] Kertész Z, Furu E, Angyal A, Freiler Á, Török K, Horváth Á. Characterization of uranium and thorium containing minerals by nuclear microscopy. J Radioanal Nucl Chem. 2015;306:283-8.
[31] Kertész Z, Szikszai Z, Uzonyi I, Simon A, Kiss ÁZ. Development of a bio-PIXE setup at the Debrecen scanning proton microprobe. Nucl Instrum Methods Phys Res. 2005;231:106-11.
[32] Bartha L, Uzonyi I. Ion beam dose measurement in nuclear microprobe using a compact beam chopper. Nucl Instr Meth B. 2000;161:339-43.
[33] Grime GW, Dawson M. Recent developments in data acquisition and processing on the Oxford scanning proton microprobe. Nucl Instr Meth B. 1995;104:107-13.
[34] Campbell JL, Boyd NI, Grassi N, Bonnick P, Maxwell JA. The Guelph PIXE software package IV. Nucl Instr Meth B. 2010;268:3356-63.
[35] Hagiwara D, Asano Y, Yamashino T, Mizuno T. Characterization of bZip-type transcription factor *AtfA* with reference to stress responses of conidia of *Aspergillus nidulans*. Biosci Biotechnol Biochem. 2008;72:2756-60.
[36] Emri T, Szarvas V, Orosz E, Antal K, Park H, Han KH, et al. Core oxidative stress response in *Aspergillus nidulans*. BMC Genomics. 2015;16:478.
[37] Orosz E, Antal K, Gazdag Z, Szabó Z, Han KH, Yu JH, et al. Transcriptome-based modeling reveals that oxidative stress induces modulation of the AtfA-dependent signaling networks in *Aspergillus nidulans*. Int J Genomics. 2017;2017:6923849.
[38] Emri T, Pócsi I, Szentirmai A. Glutathione metabolism and protection against oxidative stress caused by peroxides in *Penicillium chrysogenum*. Free Radic Biol Med. 1997;23:809-14.
[39] Emri T, Pócsi I, Szentirmai A. Analysis of the oxidative stress response of *Penicillium chrysogenum* to menadione. Free Radic Res. 1999;30:125-32.
[40] Pócsi I. Toxic metal/metalloid tolerance in fungi—a biotechnology-oriented approach. In: Bánfalvi G, editor. Cellular effects of heavy metals. Dordrecht: Springer; 2011. p. 31-58.
[41] Ramesh G, Podila GK, Gay G, Marmeisse R, Reddy MS. Different patterns of regulation for the copper and cadmium metallothioneins of the ectomycorrhizal fungus *Hebeloma cylindrosporum*. Appl Environ Microbiol. 2009;75:2266-74.
[42] Sácký J, Leonhardt T, Borovička J, Gryndler M, Briksí A, Kotrba P. Intracellular sequestration of zinc, cadmium and silver in *Hebeloma mesophaeum* and characterization of its metallothionein genes. Fungal Genet Biol. 2014;67:3-14.
[43] Hložková K, Matěnová M, Žáčková P, Strnad H, Hršelová H, Hroudová M, et al. Characterization of three distinct metallothionein genes of the Ag-hyperaccumulating ectomycorrhizal fungus *Amanita strobiliformis*. Fungal Biol. 2016;120:358-69.
[44] Khullar S, Sudhakara Reddy M. Cadmium and arsenic responses in the ectomycorrhizal fungus *Laccaria bicolor*: glutathione metabolism and its role in metal(loid) homeostasis. Environ Microbiol Rep. 2019;11:53-61.
[45] Khullar S, Reddy MS. Cadmium induced glutathione bioaccumulation mediated by γ-glutamylcysteine synthetase in ectomycorrhizal fungus *Hebeloma cylindrosporum*. BioMetals. 2019;32:101-10.
[46] Bakti F, Sasse C, Heinekamp T, Pócsi I, Braus GH. Heavy metal-induced expression of *PcaA* provides cadmium tolerance to *Aspergillus fumigatus* and supports its virulence in the *Galleria mellonella* model. Front Microbiol. 2018;13:744.
[47] Hima KA, Srinivasa RR, Vijaya SS, Jayakumar SB, Suryanarayana V, Venkateshwar P. Biosorption: an eco–friendly alternative for heavy metal removal. African J Biotechnol. 2007;6:2924-31.
[48] Wang J, Chen C. Biosorbents for heavy metals removal and their future. Biotechnol Adv. 2009;27:195-226.
[49] Gunjal AB, Kapadnis BP, Pawar NJ. Potential of live biomass of *Aspergillus* spp. in biosorption of heavy metals from aqueous solutions. J Solid Waste Technol Manag. 2017;43:216-25.
[50] Guelfi A, Azevedo RA, Lea PJ, Molina SMG. Growth inhibition of the filamentous fungus *Aspergillus nidulans* by cadmium: an antioxidant enzyme approach. J Gen Appl Microbiol. 2003;49:63-73.
[51] Guo SX, Yao GF, Ye HR, Tang J, Huang ZQ, Yang F, et al. Functional characterization of a cystathionine β-synthase gene in sulfur metabolism and pathogenicity of *Aspergillus niger* in pear fruit. J Agric Food Chem. 2019;67:4435-43.
[52] Blaudez D, Botton B, Chalot M. Cadmium uptake and subcellular compartmentation in the ectomycorrhizal fungus *Paxillus involutus*. Microbiology. 2000;146:1109-17.
[53] González-Guerrero M, Melville LH, Ferrol N, Lott JN, Azcón-Aguilar C, Peterson RL. Ultrastructural localization of heavy metals in the extraradical mycelium and spores of the arbuscular mycorrhizal fungus *Glomus intraradices*. Can J Microbiol. 2008;54:103-10.
[54] Colpaert JV, Wevers JHL, Krznaric E, Adriaensen K. How metal-tolerant ecotypes of ectomycorrhizal fungi protect plants from heavy metal pollution. Ann Forest Sci. 2011;68:17-24.
[55] Sácký J, Beneš V, Borovička J, Leonhardt T, Kotrba P. Different cadmium tolerance of two isolates of *Hebeloma mesophaeum* showing different basal expression levels of metallothionein (HmMT3) gene. Fungal Biol. 2019;123:247-54.

[56] Maenhaut W. Particle-induced X-ray emission spectrometry: an accurate technique in the analysis of biological environmental and geological samples. Anal Chim Acta. 1987;195:125-40.
[57] Tajer-Mohammad-Ghazvini P, Kasra-Kermanshahi R, Nozad-Golikand A, Sadeghizadeh M, Ghorbanzadeh-Mashkani S, Dabbagh R. Cobalt separation by *Alphaproteobacterium* MTB-KTN90: magnetotactic bacteria in bioremediation. Bioprocess Biosyst Eng. 2016;39:1899-911.
[58] Jeong BC, Hawes C, Bonthrone KM, Macaskie LE. Localization of enzymically enhanced heavy metal accumulation by *Citrobacter* sp. and metal accumulation in vitro by liposomes containing entrapped enzyme. Microbiol. 1997;143:2497-507.
[59] Koay J, Osborn RW, Grime GW, Rees S. PIXE analysis of *Fusarium culmorum* fungus treated with chemical agents. Nucl Instrum Methods Phys Res. 1996;109-10:332-5.
[60] Král J, Voltr J, Proška J, Gabriel J, Baldrian P, Černý J, et al. PIXE determination of element distribution in *Fomes fomentarius*. X-Ray Spectro. 2005;34:341-4.
[61] Weiersbye IM, Straker CJ, Przybylowicz WJ. Micro-PIXE Mapping of elemental distribution in arbuscular mycorrhizal roots of the grass, *Cynodon dactylon*, from gold and uranium mine tailings. Environ Sci Technol. 1999;37:754-60.
[62] Tarnau K, Berger A, Loewe A, Einig W, Hampp R, Chalot M, et al. Carbon dioxide concentration and nitrogen input affect the C and N storage pools in *Amanita muscaria-Picea abies* mycorrhizae. Tree Physiol. 2001;21:93-9.
[63] Wallander H, Johansson L, Pallon J. PIXE analysis to estimate the elemental composition of ectomycorrhizal rhizomorphs grown in contact with different minerals in forest soil. FEMS Microbiol Ecol. 2002;39:147-56.
[64] Olsson PA, Hammer EC, Wallander H, Pallon J. Phosphorus availability influences elemental uptake in the mycorrhizal fungus *Glomus intraradices*, as revealed by particle-induced X-ray emission analysis. Appl Environ Microbiol. 2008;74:4144-8.
[65] Hammer EC, Nasr H, Pallon J, Olsson PA, Wallander H. Elemental composition of arbuscular mycorrhizal fungi at high salinity. Mycorrhiza. 2011;21:117-29.
[66] Hammer EC, Pallon J, Wallander H, Olsson PA. Tit for tat? A mycorrhizal fungus accumulates phosphorus under low plant carbon availability. FEMS Microbiol Ecol. 2011;76:236-44.
[67] Olsson PA, Hammer EC, Pallon J, van Aarle IM, Wallander H. Elemental composition in vesicles of an arbuscular mycorrhizal fungus, as revealed by PIXE analysis. Fungal Biol. 2011;115:643-8.
[68] Turnau K, Przybyłowicz WJ, Ryszka P, Orłowska E, Anielska T, Mesjasz-Przybyłowicz J. Mycorrhizal fungi modify element distribution in gametophytes and sporophytes of a fern *Pellaeaviridis* from metaliferous soils. Chemosphere. 2013;92:1267-73.
[69] Grime GW, Pearce RB. External beam analysis of living sycamore xylem infected by pathogenic fungi. Nucl Instrum Methods Phys Res. 1995;104:299-305.
[70] Maenhaut W, de Reu L, van Rinsvelt HA, Cafmeyer J, van Espen P. Particle-induced X-ray emission (PIXE) analysis of biological materials: precision, accuracy and application to cancer tissues. Nucl Instrum Methods Phys Res. 1980;168:557-62.
[71] Sabbioni E, Kuèera J, Pietra R, Vesterberg O. A critical review on normal concentrations of vanadium in human blood, serum, and urine. Sci Total Environ. 1996;188:49-58.
[72] Kumar Ashok R, Kennedy JV, Sasikala K, Jude ALC, Ashok M, Moretto P. Trace element analysis of blood samples from mentally challenged children by PIXE. Nucl Instrum Methods Phys Res. 2002;190:449-52.

SUPPORTING INFORMATION

Additional supporting information may be found online in the Supporting Information section.

How to cite this article: Boczonádi I, Török Z, Jakab Á, et al. Increased Cd^{2+} biosorption capability of *Aspergillus nidulans* elicited by *crpA* deletion. *J Basic Microbiol*. 2020;1–11. https://doi.org/10.1002/jobm.202000112